All-optical switching with transverse optical patterns

Andrew M. C. Dawes, Lucas Illing, Joel A. Greenberg, and Daniel J. Gauthier*
Department of Physics, the Center for Nonlinear and Complex Systems, and the Fitzpatrick Institute for Photonics and Communication Systems, Duke University, Durham, North Carolina 27708, USA
(Received 17 September 2007; published 31 January 2008)

We demonstrate an all-optical switch that operates at ultra-low-light levels and exhibits several features necessary for use in optical switching networks. An input switching beam, wavelength λ, with an energy density of 10^{-2} photons per optical cross section $[\sigma=\lambda^2/(2\pi)]$ changes the orientation of a two-spot pattern generated via parametric instability in warm rubidium vapor. The instability is induced with less than 1 mW of total pump power and generates several μWs of output light. The switch is cascadable: the device output is capable of driving multiple inputs, and exhibits transistor-like signal-level restoration with both saturated and intermediate response regimes. Additionally, the system requires an input power proportional to the inverse of the response time, which suggests thermal dissipation does not necessarily limit the practicality of optical logic devices.

DOI: 10.1103/PhysRevA.77.013833 PACS number(s): 42.65.Pc, 32.80.−t, 42.65.Sf

I. INTRODUCTION

Optical switches are a crucial component of communication networks where light is redirected from channel-to-channel [1] and in general computational machines where they can act as logic elements [2]. For all-optical switches, where light controls the flow of light, there has been a continual push to increase the sensitivity of the switch so that it can be actuated with lower powers and hence decreasing the system complexity. With the advent of quantum information systems, it is important to increase the sensitivity to the point where a single switching photon is effective [3].

In a recent brief communication [4], we described an approach for achieving ultra-low-light-level all optical switching. This approach involves combining near-resonance, sub-Doppler nonlinear optics with optical pattern formation. In particular, we observe that patterns generated by a counterpropagating-beam instability can be switched with a pulse of light that has less than 3000 photons. The primary purpose of this paper is to give additional details about our experiment and to extend the work to demonstrate and characterize the transistorlike action of the switch, peform a detailed study of the time response of the switch, and to study the pattern-forming instability as various experimental parameters are varied.

The paper is structured as follows. In the next section, we review the basic requirements for a switch with classical and quantum information applications, describe previous approaches for all-optical low-light-level switching, and review the mechanisms that give rise to optical pattern formation. Section III describes our experimental system, while Sec. IV details our observations of the light generated by the pattern-forming instability. In Sec. V, we present the results of several measurements used to characterize the response of our switch to various input power levels. Finally, Sec. VI contains a discussion and analysis of these results.

II. BACKGROUND

Switches can be used in two classes of applications: information networks and computing systems. In each of these applications, information can be stored in either classical or quantum degrees of freedom. Hence the requirements for a device vary depending on the intended application.

Classical, all-optical networks require switches to reliably redirect or gate a signal depending on the presence of a control field at the device input. The switch can be either nonlatching, where the state is on only while the input is applied, or latching, where the on state persists after the input is removed. Ideally, the switch shows large contrast between on and off output levels and can be actuated by low input powers. If the network carries quantum information, the switch must be triggered by an input field containing only a single quanta (photon). Additionally, the quantum state of the transmitted signal field must be preserved.

If a switch is to be used as a logic element in a classical computing system, it must have the following characteristics: input-output isolation, cascadability, and signal level restoration [2]. Input-output isolation prohibits the device output from having back-action on the device input. Cascadability requires that a device output have sufficient power to drive the input of at least two identical devices. Signal level restoration occurs in any device that outputs a standard signal level in response to a wide range of input levels. That is, variations in the input level do not cause variations in the output level. Switching devices that satisfy these requirements are considered scalable devices, i.e., the properties of the individual device are suitable for scaling from one device to a network of many devices.

While scalability describes important properties of a switching device, sensitivity provides one way to quantify its performance. A highly sensitive all-optical switch can be actuated by a very weak optical field. Typical metrics for quantifying sensitivity are the input switching energy (in joules), the input switching energy density (in photons per optical cross section $\sigma=\lambda^2/2\pi$, where λ is the wavelength of the input beam) [5,6], and the total number of photons in the input switching pulse.

*gauthier@phy.duke.edu

One may not expect a single device to satisfy all of the requirements for these different applications. For example, a switch operating as a logic element should output a standard level that is insensitive to input fluctuations. This may be at odds with quantum switch operation where the device must preserve the quantum state of the signal field. An interesting question arises from these requirements: What happens when a classical switch is made sensitive enough to respond to a single photon? Reaching the level of single photon sensitivity has been the goal of a large body of recent work that is reviewed below.

A. Previous research on low-light-level switching

Two primary approaches to low-light-level switching have emerged, both of which seek to increase the strength of the nonlinear coupling between light and matter. The first method uses fields and atoms confined within, and strongly coupled to, a high-finesse optical cavity. The second method uses traveling waves that induce quantum interference within an optical medium and greatly enhance the effects of light on matter.

Cavity quantum-electrodynamic (QED) systems offer very high sensitivity by decreasing the number of photons required to saturate the response of an atom that is strongly coupled to a mode of the cavity. Working in the strong-coupling regime, Hood *et al.* measured the transmission of a 10 pW probe beam through a cavity with linewidth $\kappa = 40$ MHz (cavity lifetime 25 ns) while cold caesium atoms were dropped through the cavity mode. When an atom is present in the cavity mode, the effect of a single cavity photon (on average), is an order of magnitude increase in cavity transmission. For 10 cavity photons, the nonlinear optical response is saturated and almost complete transmission is observed [7]. Operating with a cavity mode waist of 15 μm, a single input photon ($\lambda = 852$ nm) represents an input energy density of $\sim 10^{-4}$ photons/σ and a total input energy of $\sim 10^{-19}$ J.

In a similar system, Birnbaum *et al.* [8] observe an effect known as photon blockade, where the absorption of a single photon prevents subsequent absorption of a second photon. For the probe frequency used in these experiments, the single-photon process is resonant with the lowest excited dressed-state of the atom-cavity system while the two-photon absorption process is suppressed. With an average of 0.21 photons in the cavity (mode waist $w = 23.4$ μm), the sensitivity of this system is $\sim 10^{-5}$ photons/σ, comparable to the lowest reported to date [9].

Although a single two-level atom in free space also exhibits an effect similar to photon blockade: Once excited it cannot immediately absorb a second photon, interactions between single photons and single atoms in free space are exceedingly difficult to control. Hence one major achievement of cavity QED is to control the single-photon, single-atom regime. The primary drawback to integrating cavity-QED-based devices into switching networks is that the cavity system is designed to operate in a single field mode, limiting the input and output channels to one per polarization. One must then discriminate between signal photons and control photons in some way other than by input mode (such as by polarization).

Of the scalability requirements for an all-optical switch, cavity QED systems do not strictly satisfy cascadability, where the output of one device must be capable of driving two ore more subsequent inputs. While coupling light to an atom contained in the cavity is efficient, all input and output signals are coupled strongly. Thus the input and the output must have similar powers, otherwise the stronger beam completely overrides the effect of the weaker beam. While cavity QED systems are well suited for controlling one single-photon signal with another single photon, they are not designed to allow single-photon inputs to control strong, many-photon signals.

A different technique for all-optical switching in cavities relies on creating and controlling cavity solitons. The most recent experiments use vertical cavity surface emitting lasers (VCSELs) as the nonlinear cavity [10]. A VCSEL can be prepared for cavity solitons by injecting a wide holding beam along the cavity axis the cavity. A narrow write beam traveling through the laser cavity induces a cavity soliton. Typically, the solitons persist until the holding beam is turned off, hence this system naturally serves as an optical memory.

Lower sensitivity is the primary limitation of the cavity soliton systems. Typical powers for the hold and write beams are 8 mW and 150 μW, respectively. The lowest reported write beam power is 10 μW for a holding beam of 27 mW, suggesting a compromise can be made to lower the required write power by increasing the hold beam power. Injecting 10 μW during the 500 ps turn-on time corresponds to an input pulse containing $\sim 24\,000$ photons, and a switching energy density of ~ 140 photons/σ (write beam diameter 10 μm, $\lambda = 960-980$ nm). Extinguishing, or switching, solitons involves either cycling the holding beam or injecting a second "write" pulse out of phase to erase the soliton, thus adding a slight complication to the device.

In terms of the scalability criteria discussed above, cavity soliton devices satisfy the requirements of signal level restoration because the soliton intensity stabilizes to a consistent level. Unlike cavity QED devices, large-area cavity soliton systems are inherently multimode and can be made very parallel with each soliton location serving as an isolated channel. To be cascadable, however, each cavity soliton would have to emit enough power to seed solitons in two or more subsequent devices. Additional techniques may then be required to properly image the output soliton into a second cavity. This problem has not been addressed in the literature to the best of our knowledge.

Traveling wave approaches can also operate with multimode optical fields and achieve few-photon sensitivity. Recent progress has been made through the techniques of electromagnetically induced transparency (EIT) [9,11–15]. As an example, Harris and Yamamoto [5] proposed a switching scheme using the strong nonlinearities that exist in specific states of four-level atoms where, in the ideal limit, a single photon at one frequency causes the absorption of light at another frequency. To achieve the lowest switching energies, the narrowest possible atomic resonances are required, which is the main challenge in implementing this proposal.

Using the narrow resonances offered by trapped cold atoms, and the Harris-Yamamoto scheme, Braje *et al.* [15] first

observed all-optical switching in an EIT medium with an input energy density of ~23 photons/σ. Subsequent work by Chen *et al.* [14] confirmed that such EIT switching operates at the 1 photon/σ level. Using a modified version of the Harris-Yamamoto scheme with an additional EIT coupling field that causes additional quantum interference, Zhang *et al.* [9] recently observed switching with ~20 photons (10^{-12} W for τ=0.7 μs with a 0.5 mm beam diameter) corresponding to 10^{-5} photons/σ. This is the highest all-optical switching sensitivity reported to date.

Although EIT switches are very sensitive, the input and output fields are necessarily of the same strength so the requirements for cascadability are not met. Additionally, the output level for EIT based switches is a monatonically decreasing function of input level [15], thus the output level is sensitive to variations in the input level and the switches do not perform signal level restoration.

Other low-light-level all-optical switching experiments have also been demonstrated recently in traveling-wave systems. By modifying the correlation between down-converted photons, Resch *et al.* [16] created a conditional-phase switch that operates at the single photon level. Using six-wave mixing in cold atoms, Kang *et al.* [17] demonstrated optical control of a field with 0.2 photons/σ with a 2 photon/σ input switching field (~10^8 input photons, over ~0.54 μs in *a* ~0.5 mm diameter beam). Both of these results exhibit high sensitivity but, like the EIT schemes, they are limited to control fields that are stronger than the output field.

Another approach combines the field enhancement offered by optical cavities with the strong coupling of coherently prepared atoms. Bistability in the output of a cavity filled with a large-Kerr, EIT medium [18] exhibits switching, but requires higher input power: ~10^8 photons/σ (0.4 mW, 80 μm radius, ~2 μs response time). Photonic crystal nanocavities have also shown bistability switching, where Tanabe *et al.* [19] demonstrated switching with 74 fJ pulses and a switching speed of <100 ps (~500 000 photons). Simulations of photonic crystal microcavities filled with an ultraslow-light EIT medium [20] suggest switching could be achieved with less than 3000 photons. Taking a different approach, Islam *et al.* [21] exploit a modulational instability in an optical fiber interferometer to gate the transmission of 184 mW by injecting only 4.4 μW (2000 photons during the 50 psec switching time). With an effective area of 2.6 $\times 10^{-7}$ cm^2, this sensitivity corresponds to 24 photons/σ.

Of the two most sensitive systems just discussed, EIT-filled photonic crystal microcavities suffer from the same drawbacks as cold-atom EIT systems: The input and output fields are required to have the same power, making them not cascadable. The other highly sensitive system, a modulational-instability fiber interferometer, is both cascadable and exhibits signal level restoration. In several ways the latter system is similar to ours: It exploits the sensitivity of instabilities and uses a sensitive detector (in their case the interferometer, in our case pattern orientation) to distinguish states of the switch.

Finally, in a very recent proposal, Chang *et al.* [22] suggest that a system consisting of a nanowire coupled to a dielectric waveguide could be used to create a single photon optical transistor. The absorption of a single photon by a two-level emitter placed close to the nanowire is sufficient to change the nanowire from complete plasmon reflection to complete plasmon transmission. This system is similar in effect to cavity QED systems, with the added advantage that the input and output are separate modes and thus separate channels. If implemented as proposed, a surface-plasmon transistor could operate with single-photon input levels, and gate signals containing many photons, thus indicating such a device would be cascadable.

Many all-optical switches have been successfully demonstrated over a period spanning several decades. However, in almost every case, one or more important features is missing from the switching device. With the requirements of scalability and sensitivity in mind, we report another approach to all-optical switching.

B. Pattern formation

Our approach to all-optical switching is to exploit collective instabilities that occur when laser beams interact with a nonlinear medium [23]. One such collective instability occurs when laser beams counterpropagate through an atomic vapor. In this configuration, given sufficiently strong nonlinear interaction strength, it is known that mirrorless parametric self-oscillation gives rise to stationary, periodic, or chaotic behavior of the intensity [24,25] and/or polarization [26–28].

Another well-known feature of counterpropagating beam instabilities is the formation of transverse optical patterns, i.e., the formation of spatial structure of the electromagnetic field in the plane perpendicular to the propagation direction [23,29]. This is also true for our experiment where a wide variety of patterns can be generated, including rings and multispot off-axis patterns in agreement with previous experiments [26,29,30].

Building an all-optical switch from transverse optical patterns combines several well-known features of nonlinear optics in a different way. Near-resonance enhancement of the atom-photon coupling makes our system sensitive to weak optical fields. Using optical fields with a counterpropagating beam geometry allows for interactions with atoms in specific velocity groups leading to sub-Doppler nonlinear optics without requiring cold atoms. Finally, using the different orientations of a transverse pattern as distinct states of a switch allows us to maximize the sensitivity of the pattern forming instability. Instabilities, by nature, are sensitive to perturbations, so, by combining instabilities with resonantly enhanced, sub-Doppler nonlinearities, we created a switch with very high sensitivity.

III. EXPERIMENTAL SETUP

Previous observations of pattern-forming instabilities have required several to hundreds of milliwatts of optical power due to the typically weak nonlinear interactions and the correspondingly high threshold for self-oscillation. To lower the instability threshold, we tune the pump laser close to an atomic resonance, and use a pump beam polarization configuration that gives rise to polarization instabilities

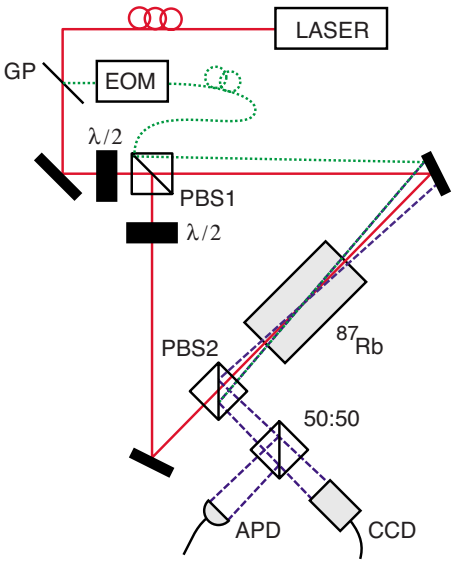

FIG. 1. (Color online) Experimental setup for transverse optical pattern generation. A cw Ti:sapphire laser serves as the light source. Optical elements are as follows: Uncoated glass plate (GP), electro-optic modulator (EOM), half-wave plates ($\lambda/2$), polarizing beam splitters (PBS1, PBS2), 50/50 beam splitter (50:50), CCD (charge-coupled device) camera (CCD), and avalanche photodiode (APD). Beams are indicated by line type: Pump beams (solid), switch beam (dotted), and instability-generated light (dashed). The foward (backward) pump beam propagates in the cw (ccw) direction through the triangular ring cavity.

which are known to have lower self-oscillation thresholds [31]. The low instability threshold reduces the power required to generate optical patterns and gives rise to patterns that exhibit sensitivity to perturbation by a weak probe beam, as discussed in Sec. V and Ref. [4].

A diagram of our experimental setup is shown in Fig. 1. Two beams of light from a common laser source counterpropagate through warm rubidium vapor contained in a glass cell. The light source is a frequency-stabilized continuous-wave Ti:sapphire laser, the output of which is spatially filtered using a single-mode optical fiber with an angled entrance face and a flat-polished exit face. The beam is then roughly collimated to a spot size ($1/e$ field radius) of $w = 340\ \mu$m with the beam waist located at the center of the vapor cell. The power ratio between the pump beams is controlled by a half-wave plate at the input of the first polarizing beam splitter (PBS1). We denote the beam passing through PBS1 as the forward beam and the reflected beam as the backward beam. A second half-wave plate in the backward beam path rotates the polarization such that the pump beams are linearly polarized with parallel polarizations.

The atomic medium is isotopically enriched rubidium vapor (>90% ^{87}Rb), which is contained in a 5-cm-long glass cell heated to 67 °C (corresponding to an atomic number density of $\sim 2\times 10^{11}$ atoms/cm^3). The cell is tilted with respect to the incident laser beams to prevent possible oscillation between the uncoated windows. The cell has no paraffin coating on the interior walls that would prevent depolarization of the ground-state coherence, nor does it contain a buffer gas that would slow diffusion of atoms out of the pump laser beams. The Doppler-broadened linewidth of the transition at this temperature is ~550 MHz. To prevent the occurrence of magnetically induced instabilities and reduce Faraday rotation, we use a Helmholtz coil to cancel the ambient magnetic field component along the direction of the counterpropagating laser beams.

A polarizing beam splitter (PBS2) placed in the beam path separates light polarized orthogonally to the pump beam. This light, henceforth referred to as *output* light, is subsequently split with a 50:50 beam splitter and then observed simultaneously using any two of the following: A CCD camera (Marshall V-1050A), an avalanche photodiode (Hamamatsu C5460), or a photomultiplier tube (Hamamatsu H6780-20) as shown in Fig. 1.

For measurements of the switch response, as discussed in Sec. V, we inject a weak beam at a small angle to the pump beams. This switch beam is indicated in Fig. 1 by a dotted line. An uncoated glass plate reflects ~4% of the pump beam power into a fiber coupler and through a high-speed fiber-based Mach-Zehnder amplitude modulator (EOSpace Lithium Niobate Modulator, AZ-2K1-20-PFU-SFU-770, 20 GHz bandwidth). Neutral density filters placed before the EOM are used to reduce the switch beam power to the range 0.1–1 nW. The switch beam then enters PBS1 near the pump beams, propagates in the forward direction at a small angle (<5 mrad) to the forward pump beam, and crosses both pump beams in the center of the vapor cell.

IV. CHARACTERISTICS OF THE INSTABILITY-GENERATED LIGHT

In our setup, the counterpropagating pump beams give rise to a supercritical instability that generates new light when the pump power is above a certain threshold. For our experimental setup, we observe instability generated light (output light) in the state of polarization orthogonal to that of the pump beams and with the same frequency as the pump beams.

We find that the power of the output light is maximized (and the threshold for this instability is lowest) when the frequency of the pump beams is set near an atomic resonance, i.e., the instability occurs near either the D_1 or D_2 transition of ^{87}Rb. For the remainder of the paper, we describe results for pump-beam frequencies near the D_2 transition ($^5S_{1/2} \rightarrow {}^5P_{3/2}$, 780 nm wavelength).

Figure 2(c) shows the power of the output light as a function of pump frequency detuning, defined as $\Delta = \nu - \nu_{F=1,F'=1}$. We observe several sub-Doppler features, where the maximum power emitted in the orthogonal polarization occurs when the laser frequency ν is tuned $\Delta = +25$ MHz. For this detuning, 3 μW of output light is generated, indicating that ~1% of the incident pump power is being converted to the orthogonal polarization. Because the detuning is small relative to the doppler width, most of the pump light is absorbed by the medium. Of the 80 μW of pump light transmitted in the forward direction, ~4% is being converted to the orthogonal polarization. For a fixed detuning, the generated power does not exhibit bistability as the pump power is increased and then decreased.

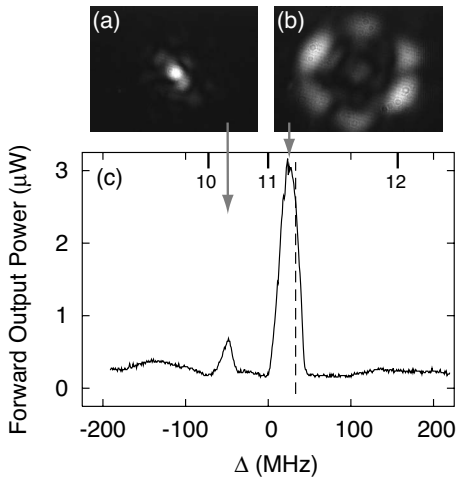

FIG. 2. Instability-generated patterns and optical power as a function of pump laser frequency detuning ($\Delta=\nu-\nu_{F=1,F'=1}$). (a),(b) Patterns for red and blue pump laser detunings ($\Delta=-50$ MHz and $\Delta=+25$ MHz, respectively, indicated by arrows). (c) Orthogonally polarized output power, emitted in the forward direction, as a function of frequency. These data correspond to a single scan through the $^5S_{1/2}(F=1)\rightarrow{}^5P_{3/2}(F')$ transition in ^{87}Rb from low to high frequency. The bold tick marks indicate the hyperfine transitions labeled by FF′, where F (F′) is the ground (excited) state quantum number. Our switching experiments are conducted with the pump laser detuned $\Delta=+30$ MHz (dashed line). Pump beam power levels: 630 μW forward and 225 μW backward.

The light generated in our system shows structure in the transverse plane. We find that the output light is emitted in the forward and backward direction along cones centered on the pump beams [see Fig. 3(a)]. The angle between the pump-beam axis and the cone is on the order of ~5 mrad and can be understood as arising from competition between two different nonlinear processes: backward four-wave mixing in the phase-conjugation geometry and forward four-wave mixing [32].

We observe the cross-polarized off-axis output light on a measurement plane perpendicular to the propagation direction and in the far field. Figure 2 shows a sample of the transverse patterns as a function of pump frequency detuning

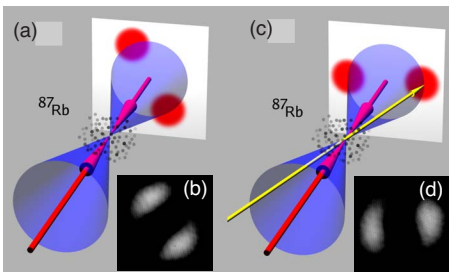

FIG. 3. (Color online) Generated light is emitted along cones (blue), which are centered on the pump beams (red), and forms a transverse pattern (red spots) in the measurement plane. (a) Unperturbed system with two-spot pattern induced via weak pump-beam misalignment; (b) data showing two-spot pattern. (c) A weak switch beam (yellow) rotates the pattern; (d) data showing rotated pattern.

for pump powers above the instability-threshold. For pump beams that are red-detuned ($\Delta=-50$ MHz) the instability occurs on-axis, leading to a pattern containing one spot centered on the pump beam axis [Fig. 2(a)]. For blue-detuned pump beams ($\Delta=25$ MHz) the instability occurs off-axis and the conical emission is apparent from the hexagon pattern of the transverse field as shown in Fig. 2(b). Conical emission occurs only for blue-detuned beams where the sign of the nonlinear refractive index is positive [32–34]. The rotational symmetry, expected for conical emission, is spontaneously broken resulting in the formation of a hexagon pattern in the far field [35]. The origin of the hexagonal pattern can be described by four-wave mixing where each spot on the hexagon is the result of a parametric process that annihilates one off-axis photon and one pump photon and creates two off-axis photons, both with wave vectors corresponding to the two next-nearest spots in the hexagon [33]. It should also be noted that the hexagonal symmetry is slightly broken by variations in the surface of the glass vapor cell and other experimental imperfections, even for well-aligned pump beams. This is manifested in the preferred azimuthal angle of emission: The upper-left and lower-right lobes of Fig. 2(b) are brighter than the other lobes.

This weak symmetry breaking can be made stronger by introducing a slight amount, less than 1 mrad, of misalignment between the pump beams. Doing so results in a two-spot pattern for pump beams just above threshold and detuned $\Delta=+25$ MHz [see Fig. 3(b)]. The azimuthal orientation angle of these spots is stable for several minutes and is reproduced upon turning the pump beams off and on. The orientation can be influenced by the misalignment of the pump beams, application of a weak magnetic field or by injecting a weak probe beam, as discussed in Sec. V.

In addition to exhibiting pattern formation, the instability observed in our system has a very low threshold. The instability-threshold determines the lowest pump power for which output light is generated. A common way to quantify the instability threshold for a setup with counterpropagating beams is to fix the power of one of the beams and measure the output power as a function of the power in the second pump beam [13,27]. For a pump-beam detuning of $\Delta=+25$ MHz and with a fixed forward pump power of 630 μW, we find that the backward pump power threshold is ~125 μW, corresponding to a total pump power of 755 μW.

Another way to measure the instability threshold is to determine the minimum total pump power necessary to generate output light. Figure 4 shows the result of such a measurement for our experiment. We find that there is an optimum ratio of forward power to backward power of ~2.7-to-1. At this ratio, we determine the threshold for off-axis emission to be 600 μW which is slightly lower than the threshold measured with fixed forward beam power. Also shown in Fig. 4, for comparison, are data for the on-axis instability, detuning $\Delta=-50$ MHz, with a higher threshold of 1.1 mW.

Both threshold measures demonstrate that the nonlinear process that generates new light is induced by a pair of very weak fields indicating very strong nonlinear matter-light

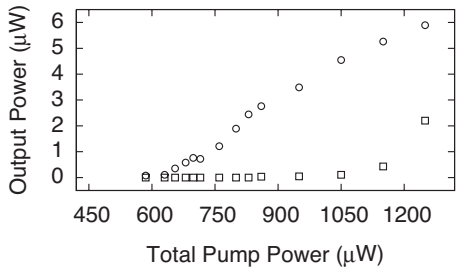

FIG. 4. Instability thresholds. Generated optical power as a function of total pump beam power. The off-axis instability occurs with a threshold of 600 μW (circles) whereas the on-axis instability occurs with a threshold of 1.1 mW (squares). Data shown corresponds to a fixed pump beam power ratio of 2.7 to 1 (forward to backward).

interaction comparable with the best reported results to date for warm-vapor counterpropagating beam systems [13].

For most of the early observations of nearly-degenerate instabilities, strong pump fields were used (typically hundreds of mW) [29,30,36]. A considerably higher threshold was reported in a previous work by one of us for polarization instabilities in a sodium vapor [27], where a threshold of tens of mW was found when the pump fields were tuned near an atomic resonance. More recently, Zibrov *et al.* [13] observed parametric self-oscillation with pump powers in the μW regime using a more involved experimental setup ("double-Λ" configuration) designed specifically to lower the instability threshold. In their experiment, atomic coherence effects increase the nonlinear coupling efficiency. They report oscillation with as little as 300 μW in the forward beam. With 5 mW of forward-beam power, their instability threshold corresponds to 20 μW in the backward beam. In contrast, the results reported here demonstrate that spontaneous parametric oscillations are induced by μW-power counterpropagating pump beams without the need for special coherent preparation of the medium. Furthermore, Zibrov *et al.* observe only on-axis emission, whereas, with our pump beam configuration, we find that off-axis emission requires roughly half as much pump power as on-axis emission. In situations where low power and high sensitivity are important, such as in all-optical switching, the lower instability threshold may make off-axis instabilities preferable.

V. SWITCHING TRANSVERSE PATTERNS

We find the azimuthal angle of the instability-generated beams is extremely sensitive to perturbations because the symmetry breaking of our setup is small. The preferred azimuthal orientation of the pattern can be overcome by injecting a weak switching beam along the cone of emission at a different azimuth as shown in Fig. 3(c). Typically, this causes the pattern to rotate such that one spot is aligned to the switching beam with essentially no change in the total power of the pattern.

To quantify the dynamic behavior of the switch, we inject a series of pulses by turning the switch beam on and off with the Mach-Zehnder amplitude modulator. Spatially filtering

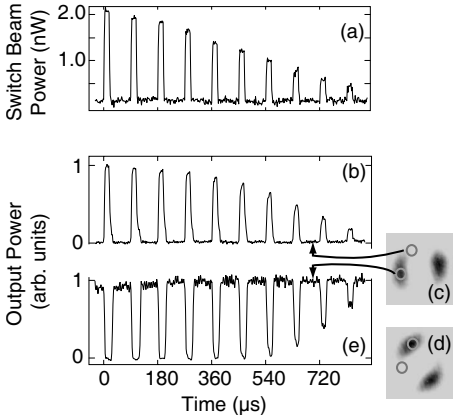

FIG. 5. Time response of the pattern. (a) While turning the switch beam on and off with successively decreasing power levels, (c), (d) two detectors simultaneously measure the spatial regions indicated on the center frames by circles which encompass bright and dark areas of the output pattern (the images have been inverted for visibility). These images are collected by CCD camera and the normalized detector output signals are shown in (b), (e) corresponding to the spatial location of the detector within the pattern. (b) The "on-state" detector and (e) The "off-state" detector.

the output pattern enables direct measurement of the switch behavior. High-contrast switching is confirmed by simultaneously measuring two output spots, one corresponding to a bright spot that exists in the absence of the switch beam [off state, lower circle in Figs. 5(c) and 5(d)] and the other corresponding to a spot that exists when the switch beam is present [on state, upper circle in Figs. 5(c) and 5(d)]. The alternating signals shown in Figs. 5(b) and 5(e) demonstrate switching of the power from one switch state to another with high contrast.

We inject switch beam pulses that steadily decrease in power, which allows us to sample the response of the system to various input levels. One notable feature of the system response is the transition from complete switching to partial switching. The first six pulses in Fig. 5 show that the on-state detector [Fig. 5(b)] is fully illuminated and the off-state detector [Fig. 5(e)] is dark. This indicates that the switch beam has caused complete rotation of the pattern and transferred all of the power from the off-state spots to the on-state spots. For the last four pulses in the series, the system exhibits partial switching, where the on-state detector is only partially illuminated and the off-state detector is partially darkened. This partial response indicates that the off-state spots are suppressed but not extinguished when the switch beam is applied with less than 1 nW. Similarly the on-state spots are generated but not at full power. In this intermediate regime, from 1 nW to 200 pW, the response is linearly proportional to the input power. Input powers below 200 pW do not rotate the spots so the output remains in the off state.

Also visible in Fig. 5(e) is a weak secondary modulational instability that causes oscillations in the total output power. These oscillations are most visible in the off-state detector [Fig. 5(e)] when the switch beam is not present. Experimental noise, primarily due to the detection electronics, is barely visible in this trace, hence the majority of the signal variation

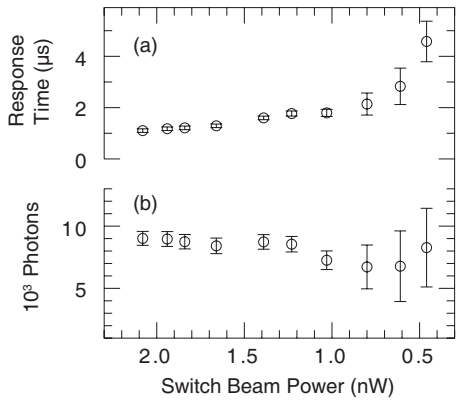

FIG. 6. Response time and number of input photons as a function of switch beam power. (a) The response time increases for decreasing switch beam power. (b) The increased response time for weak input powers indicates that a constant number of photons are required to actuate the switch regardless of the amount of input power.

is due to this modulational instability. Fortunately, the effects of this secondary instability are minor, the primary effect being an increase in the switch response time uncertainty, as discussed below.

Finally, we do not observe bistability in the switch response for the experimental situation described here. The state of the switch is on only while the switch beam is being applied, thus no latching occurs. For other experimental conditions with slightly different pump-beam alignment and longer duration switch-beam pulses, a small degree of latching was observed previously [4].

VI. DISCUSSION

To quantify the sensitivity of the system, we measure the response time and from this calculate the number of photons required to actuate the switch. We define the response time of the device as the time between the initial rising edge of the switch beam pulse and the point where the on-spot signal crosses a threshold level set to correspond to a signal-to-noise ratio of 1. As shown in Fig. 6(a), the measured response time increases as the input switch beam power decreases.

The number of photons required to actuate the switch is given by $N_p = \tau P_s / E_p$ where τ is the response time, P_s is the switch beam power and $E_p = 2.54 \times 10^{-19}$ J is the photon energy. For the ten switch-beam powers corresponding to Fig. 5(a), the number of switching photons is plotted in Fig. 6(b). The response time is longer for weak switch-beam powers so the photon number remains roughly constant, in the range between 6000 and 9000, regardless of the input power level. The noticeable increase in uncertainty for the latter points of Fig. 6(a) is primarily due to the weak secondary modulational instability in the system. For weak input powers, the switch responds more quickly when the input pulse arrives in phase with the oscillations due to this instability. The error bars represent the range of response times observed. One goal of our future work is to minimize the effect of this secondary instability.

To compare the sensitivity of our switch to those previously discussed, we evaluate the energy density in photons per σ. For the switching beam spot size used, ($1/e$ field radius) $w_0 = 235$ μm, 8000 switching photons correspond to a switching beam energy density of 10^{-2} photons/σ. Therefore, both EIT-based switches [9] and our pattern-based switch have surpassed the minimum value (1 photon/σ) originally expected for optical logic operations [6]. Both approaches operate at very low light levels, although our system is markedly simpler than cold-atom EIT systems or cavity QED systems, requiring only one optical frequency and occurring in warm atomic vapor.

In addition to exhibiting high sensitivity, our switch is cascadable, with an output power capable of driving many subsequent devices. The 3 μW output power is sufficient to actuate over 1000 similar switches, with each requiring $\sim$1 nW of input power.

The performance and scalability of a logic element can be further characterized by the device power requirements. In an early paper addressing the physical limits of logic devices, Keyes determined that optical logic based on the saturation of a two-level atomic transition requires input power levels that scale as $P \propto 1/\tau^2$ where P is the power required to complete one logic operation and τ is the response time of the device [6]. This result leads to the conclusion that optical logic elements face thermal dissipation limits at lower speeds than electronic logic elements do, thus reducing their practical range of application.

A constant number of switching photons, however, implies that the power requirements of our device follows $P \propto 1/\tau$ rather than $P \propto 1/\tau^2$. For response times below 10^{-8} s this is lower than the best-case estimate for an optical logic element based on saturating a two-level transition [6]. This new scaling law for required power with response time indicates that the thermal dissipation limits previously assumed for optical logic devices are not as severe for our pattern-based switch and may extend the usability of optical logic to faster, more compact devices than was previously thought.

Finally, the two response regimes exhibited by our switch indicate that the output satisfies the conditions for signal level restoration. For a device to exhibit signal level restoration, variations in the input level cannot cause variations in the output level. In every device, however, there is a narrow range of input levels, known as the intermediate region, that lead to intermediate output levels. For input levels above or below the intermediate range the output is *saturated* as a logic high or low respectively. In the case of our device, this intermediate region is between 200 pW and 1 nW. For input levels below 200 pW, the output is low, and for input levels above 1 nW, the output is high with a level set by the pump beam power.

Signal level restoration is a key property of the electronic transistor and this demonstration of an optical logic element that exhibits level restoration is a key step towards practical optical switches. An all-optical transistor would have applications in many data processing and communication networks in the future.

VII. CONCLUSION

Instabilities that give rise to the generation of transverse optical patterns are induced in a simple atomic vapor system with less than 1 mW of pump power. These results suggest that coherently prepared media are not necessary for the observation of nonlinear optical interactions at low light levels. The sensitivity of these instabilities to perturbations enables incredibly weak optical fields to control the direction of much stronger beams generated by the instability. These patterns demonstrate low-light-level nonlinear optics using a simple setup and enable another kind of all-optical switch that satisfies the requirements of scalability.

Other recent all-optical switches are based on quantum interference or cavity QED and require complex experimental environments to operate with a sensitivity of less than one photon per atomic cross section. Furthermore, previous devices fail to meet one or more of the criteria for scalability. We have extended our previous demonstration of a cascadable, pattern-based all-optical switch that operates at ultralow-light levels. The results presented here show that such a switch exhibits the transistorlike behavior of signal level restoration, and is operated in a very simple experimental environment with <1 mW of total pump power.

ACKNOWLEDGMENTS

We gratefully acknowledge the financial support of the U.S. Army Research Office Grant No. W911NF-05-1-0228 and the DARPA DSO Slow-Light Program.

[1] H. M. Gibbs, *Optical Bistability: Controlling Light with Light* (Academic Press, Orlando, 1985).
[2] R. W. Keyes, J. Phys.: Condens. Matter **18**, S703 (2006).
[3] D. Bouwmeester, A. K. Ekert, and A. Zeilinger, *The Physics of Quantum Information: Quantum Cryptography, Quantum Teleportation, Quantum Computation* (Springer, Berlin, 2000).
[4] A. M. C. Dawes, L. Illing, S. M. Clark, and D. J. Gauthier, Science **308**, 672 (2005).
[5] S. E. Harris and Y. Yamamoto, Phys. Rev. Lett. **81**, 3611 (1998).
[6] R. W. Keyes, Science **168**, 796 (1970).
[7] C. J. Hood, M. S. Chapman, T. W. Lynn, and H. J. Kimble, Phys. Rev. Lett. **80**, 4157 (1998).
[8] K. Birnbaum, A. Boca, R. Miller, A. Boozer, T. Northup, and H. Kimble, Nature (London) **436**, 87 (2005).
[9] J. Zhang, G. Hernandez, and Y. Zhu, Opt. Lett. **32**, 1317 (2007).
[10] X. Hachair, L. Furfaro, J. Javaloyes, M. Giudici, S. Balle, J. Tredicce, G. Tissoni, L. A. Lugiato, M. Brambilla, and T. Maggipinto, Phys. Rev. A **72**, 013815 (2005).
[11] S. E. Harris, Phys. Today **50**, 36 (1997).
[12] H. Schmidt and A. Imamoglu, Opt. Lett. **21**, 1936 (1996).
[13] A. S. Zibrov, M. D. Lukin, and M. O. Scully, Phys. Rev. Lett. **83**, 4049 (1999).
[14] Y.-F. Chen, Z.-H. Tsai, Y.-C. Liu, and I. A. Yu, Opt. Lett. **30**, 3207 (2005).
[15] D. A. Braje, V. Balić, G. Y. Yin, and S. E. Harris, Phys. Rev. A **68**, 041801(R) (2003).
[16] K. J. Resch, J. S. Lundeen, and A. M. Steinberg, Phys. Rev. Lett. **89**, 037904 (2002).
[17] H. Kang, G. Hernandez, and Y. Zhu, Phys. Rev. Lett. **93**, 073601 (2004).
[18] H. Wang, D. Goorskey, and M. Xiao, Phys. Rev. A **65**, 051802(R) (2002).
[19] T. Tanabe, M. Notomi, S. Mitsugi, A. Shinya, and E. Kuramochi, Opt. Lett. **30**, 2575 (2005).
[20] M. Soljačić, E. Lidorikis, J. D. Joannopoulos, and L. V. Hau, Appl. Phys. Lett. **86**, 171101 (2005).
[21] M. Islam, S. Dijaili, and J. Gordon, Opt. Lett. **13**, 518 (1988).
[22] D. E. Chang, A. S. Sorensen, E. A. Demler, and M. D. Lukin, Nature Physics, advance online publication, 26 August 2007 (doi:10.1038/nphys708) (2007).
[23] L. A. Lugiato, Chaos, Solitons Fractals, **4**, 1251 (1994).
[24] Y. Silberberg and I. Bar-Joseph, J. Opt. Soc. Am. B **1**, 662 (1984).
[25] G. Khitrova, J. F. Valley, and H. M. Gibbs, Phys. Rev. Lett. **60**, 1126 (1988).
[26] D. J. Gauthier, M. S. Malcuit, A. L. Gaeta, and R. W. Boyd, Phys. Rev. Lett. **64**, 1721 (1990).
[27] D. J. Gauthier, M. S. Malcuit, and R. W. Boyd, Phys. Rev. Lett. **61**, 1827 (1988).
[28] A. L. Gaeta, R. W. Boyd, J. R. Ackerhalt, and P. W. Milonni, Phys. Rev. Lett. **58**, 2432 (1987).
[29] A. Petrossian, M. Pinard, A. Maître, J. Y. Courtois, and G. Grynberg, Europhys. Lett. **18**, 689 (1992).
[30] G. Grynberg, E. Le Bihan, P. Verklerk, P. Simoneau, J. R. R. Leite, D. Bloch, S. Le Boiteux, and M. Ducloy, Opt. Commun. **67**, 363 (1988).
[31] A. L. Gaeta and R. W. Boyd, Phys. Rev. A **48**, 1610 (1993).
[32] G. Grynberg and J. Paye, Europhys. Lett. **8**, 29 (1989).
[33] G. Grynberg, Opt. Commun. **66**, 321 (1988).
[34] W. J. Firth and C. Paré, Opt. Lett. **13**, 1096 (1988).
[35] J. B. Geddes, R. A. Indik, J. V. Moloney, and W. J. Firth, Phys. Rev. A **50**, 3471 (1994).
[36] A. Maître, A. Petrossian, A. Blouin, M. Pinard, and G. Grynberg, Opt. Commun. **116**, 153 (1995).